C. R. Mecanique 341 (2013) 616–624

Contents lists available at SciVerse ScienceDirect

Comptes Rendus Mecanique

www.sciencedirect.com

New nonlinear multi-scale models for wrinkled membranes

Noureddine Damil [a], Michel Potier-Ferry [b,c,*], Heng Hu [d]

[a] Laboratoire d'ingénierie et matériaux, LIMAT, faculté des sciences Ben M'Sik, université Hassan II Mohammedia Casablanca, Sidi Othman, Casablanca, Morocco
[b] Laboratoire d'études des microstructures et de mécanique des matériaux, LEM3, UMR CNRS 7239, université de Lorraine, île du Saulcy, 57045 Metz cedex 01, France
[c] Laboratory of Excellence on Design of Alloy Metals for Low-Mass Structures (DAMAS), université de Lorraine, France
[d] School of Civil Engineering, Wuhan University, 8 South Road of East Lake, 430072 Wuhan, PR China

ARTICLE INFO

Article history:
Received 10 May 2013
Accepted 18 June 2013
Available online 24 July 2013

Keywords:
Wrinkling
Membrane
Slowly variable Fourier coefficients
Multi-scale

ABSTRACT

A new macroscopic approach to the modelling of membrane wrinkling is presented. Most of the studies of the literature about membrane behaviour are macroscopic and phenomenological, the influence of wrinkles being accounted for by nonlinear constitutive laws without compressive stiffness. The present method is multi-scale and it permits to predict the wavelength and the spatial distribution of wrinkling amplitude. It belongs to the family of Landau–Ginzburg bifurcation equations and especially relies on the technique of Fourier series with slowly varying coefficients. The result is a new family of macroscopic membrane models that are deduced from Föppl–von Kármán plate equations. Numerical solutions are presented, giving the size of the wrinkles as a function of the applied compressive and tensile stresses.

1. Introduction

Two main classes of numerical approaches are currently used to model membrane mechanical behaviour and wrinkling. The first class of methods is based on elastic shell models; see for instance [1–4]. Nowadays, many commercial finite-element codes allow us to carry out such nonlinear shell computations. The advantage of shell analyses is their capacity to describe the details of the membrane response: instability threshold, size, wavelength, and orientation of the wrinkles. As a counterpart, the numerical model is heavy and especially very difficult to control in cases with many wrinkles, what leads generally to many equilibrium solutions. These full models will be referred to as "microscopic models" because their finite-element discretisation provides a detailed response at the scale of the wrinkles.

With the second group of numerical methods, one does not intend to fully describe the wrinkles, but only the decrease of stress they generate. The bending stiffness is neglected and wrinkling is accounted for indirectly by a nonlinear constitutive law of unilateral type, where the compressive stresses are eliminated [5,6]. Two variants have to be mentioned: first, the method of Roddeman [7], which splits the deformation gradient into consistent membrane part and wrinkling part [8–11]; second, models with an internal length, like Cosserat theory [12,13], which avoids any loss of ellipticity in the case of compressive stresses. These models can be considered as macroscopic ones and indeed they require much less refined meshes than the previous ones, because the size of the macroscopic finite elements is not related to size of the wrinkles.

In this paper, macroscopic models of membranes including wrinkling are deduced from the fine plate model without any phenomenological assumptions. The bending stiffness effects are included, not only to define the wrinkling wavelength, but

* Corresponding author at: Laboratoire d'études des microstructures et de mécanique des matériaux, LEM3, UMR CNRS 7239, université de Lorraine, île du Saulcy, 57045 Metz cedex 01, France.

E-mail addresses: noureddine.damil@univh2m.ma (N. Damil), michel.potier-ferry@univ-lorraine.fr (M. Potier-Ferry), huheng@whu.edu.cn (H. Hu).

1631-0721/$ – see front matter
http://dx.doi.org/10.1016/j.crme.2013.06.001

also to predict the macroscopic evolution of the wrinkling pattern. The idea is to build a theory coupling pure membrane model with an envelope equation as in the Landau–Ginzburg approach [14,15]. Nevertheless we shall not apply the classical Landau–Ginzburg asymptotic technique, which is valid only near the bifurcation, but a variant where the nearly periodic fields are represented by Fourier series with slowly varying coefficients [16–19]. In other words, we use a multi-scale method whose result is a generalised continuum including an internal length and where the macroscopic stresses are Fourier coefficients of the microscopic stress. The resulting models are macroscopic and require only rough meshes, because their unknowns are in-plane displacements and slowly varying envelopes of the wrinkles.

For the sake of simplicity, we limit ourselves to plane membrane, the fine model being the traditional Föppl–von Kármán plate equations. Two examples assess the model's ability to represent the behaviour of membranes in the presence of wrinkling.

2. Nonlinear macroscopic models of wrinkling

2.1. The full model

The well-known Föppl–von Kármán equations for elastic isotropic plates will be considered as the reference model in this paper:

$$\begin{cases} D\Delta^2 w - \operatorname{div}(\mathbf{N}\nabla w) = 0 \\ \mathbf{N} = \mathbf{L}^m \cdot \boldsymbol{\gamma} \\ 2\boldsymbol{\gamma} = \nabla \mathbf{u} + {}^t\nabla \mathbf{u} + \nabla w \otimes \nabla w \\ \operatorname{div} \mathbf{N} = 0 \end{cases} \tag{1}$$

where $\mathbf{u} = (u, v) \in \mathbb{R}^2$ is the in-plane displacement, w is the deflection, $\mathbf{N}$ and $\boldsymbol{\gamma}$ are the membrane stress and strain. With the vectorial notations $(\mathbf{N} \to {}^t(N_X\ N_Y\ N_{XY}), \boldsymbol{\gamma} \to {}^t(\gamma_X\ \gamma_Y\ 2\gamma_{XY}))$, the membrane elasticity tensor is represented by the matrix:

$$\frac{Et}{1-\nu^2}\begin{bmatrix} 1 & \nu & 0 \\ \nu & 1 & 0 \\ 0 & 0 & \frac{1-\nu}{2} \end{bmatrix}$$

The corresponding energy $\mathcal{E}$ can be split into a membrane part $\mathcal{E}_{\text{mem}}$ and a bending part $\mathcal{E}_{\text{ben}}$, as follows:

$$\begin{cases} \mathcal{E}(\mathbf{u}, w) = \mathcal{E}_{\text{ben}}(w) + \mathcal{E}_{\text{mem}}(\mathbf{u}, w) \\ 2\mathcal{E}_{\text{ben}}(w) = D \displaystyle\iint \left((\Delta w)^2 - 2(1-\nu)\left(\frac{\partial^2 w}{\partial X^2}\frac{\partial^2 w}{\partial Y^2} - \left(\frac{\partial^2 w}{\partial X \partial Y}\right)^2 \right) \right) \mathrm{d}\omega \\ 2\mathcal{E}_{\text{mem}}(\mathbf{u}, w) = \displaystyle\iint \boldsymbol{\gamma} \cdot \mathbf{L}^m \cdot \boldsymbol{\gamma}\, \mathrm{d}\omega = \frac{Et}{1-\nu^2} \iint \left(\gamma_X^2 + \gamma_Y^2 + 2(1-\nu)\gamma_{XY}^2 + 2\nu\gamma_X\gamma_Y \right) \mathrm{d}\omega \end{cases} \tag{2}$$

2.2. A multi-scale approach using the Fourier coefficient

We adapt in this 2D framework the method of Fourier series with slowly variable coefficients [17]. For simplicity, we suppose that the instability wavenumber Q is known and we only consider wrinkles in the OY-direction. Within this method, the unknown field $\mathbf{U}(X, Y) = (\mathbf{u}(X, Y), w(X, Y), \mathbf{N}(X, Y), \gamma(X, Y))$, whose components are in-plane displacement, transverse displacement, membrane stress and strains, is written in the following form:

$$\mathbf{U}(X, Y) = \sum_{m=-\infty}^{+\infty} \mathbf{U}_m(X, Y) \exp(\mathrm{i}mQX) \tag{3}$$

where the new macroscopic unknown fields $\mathbf{U}_m(X, Y)$ vary slowly on a single period $[X, X + \frac{2\pi}{Q}]$ of the oscillation pattern. Of course, we do not need an infinite number of Fourier coefficients and we limit ourselves to three harmonics: the mean field $\mathbf{U}_0(X, Y)$ and the envelope of the oscillations $\mathbf{U}_1(X, Y)\mathrm{e}^{\mathrm{i}QX}$, $\bar{\mathbf{U}}_1(X, Y)\mathrm{e}^{-\mathrm{i}QX}$. According to [17], the second harmonic should be taken into account to recover the results of the Landau–Ginzburg bifurcation approach. Nevertheless, the rapid one-dimensional oscillations $\mathrm{e}^{\mathrm{i}QX}$ are inextensional, so that they do not contribute to the membrane energy. The macroscopic model with the second harmonic has been established, but within the approximation of [17, §4.1], we have shown that $\mathbf{N}_2 = 0$, $w_2 = 0$, so that the second harmonic does not influence the macroscopic model. The details of this calculation are omitted.

In principle, the mean field $\mathbf{U}_0(X, Y)$ is real and the envelope $\mathbf{U}_1(X, Y)$ is complex-valued, but spatial evolutions of the patterns can be reasonably accounted for with only two real coefficients: for practical finite-element calculations, this simplification of two real unknowns will be done, even if a complex envelope can improve the treatment of boundary conditions [19].

The derivation rules are straightforward [16] and, in a first time, the derivatives of the envelopes are not neglected. For instance, the first Fourier coefficient of the gradient of the deflection is given by:

$$\{(\nabla w)_1\} = \left\{ \begin{array}{c} \frac{\partial w_1}{\partial X} + \mathrm{i} Q\, w_1 \\ \frac{\partial w_1}{\partial Y} \end{array} \right\} \tag{4}$$

2.3. Macroscopic membrane energy

We now derive the macroscopic model and we begin with the membrane effects. We apply the principles established in [16,17]. The derivatives are computed exactly as in Eq. (4), but some simplifications will be added to obtain the simplest macroscopic model having the same internal length as the asymptotic Landau–Ginzburg approach. Next, one could deduce the macroscopic model by identifying the Fourier coefficients in the differential equations (1), but a most convenient approach consists in retaining only the harmonic of level zero to approximate an energy density:

$$\iint\limits_{\text{period}} h \,\mathrm{d}\omega \approx \iint\limits_{\text{period}} h_0 \,\mathrm{d}\omega \tag{5}$$

where h_0 represents the harmonic zero of the density h. The rule (5) is a consequence of the assumption of slowly varying envelopes. For instance, the energy due to a higher harmonic vanishes if the envelope is assumed to be constant on a period:

$$\iint\limits_{\text{period}} h_m(X,Y)\exp(\mathrm{i}mQx)\,\mathrm{d}\omega \approx h_m(X,Y)\iint\limits_{\text{period}} \exp(\mathrm{i}mQx)\,\mathrm{d}\omega = 0 \tag{6}$$

First, we compute the mean value or the harmonic zero of the Lagrange strain, by using Eq. (4) and without any approximation:

$$\{\gamma_0\} = \left\{ \begin{array}{c} \gamma_{X0} \\ \gamma_{Y0} \\ 2\gamma_{XY0} \end{array} \right\} = \left\{ \begin{array}{c} \frac{\partial u_0}{\partial X} + \frac{1}{2}(\frac{\partial w_0}{\partial X})^2 + |\frac{\partial w_1}{\partial X} + \mathrm{i}Q\,w_1|^2 \\ \frac{\partial v_0}{\partial Y} + \frac{1}{2}(\frac{\partial w_0}{\partial Y})^2 + |\frac{\partial w_1}{\partial Y}|^2 \\ \frac{\partial u_0}{\partial Y} + \frac{\partial v_0}{\partial X} + \frac{\partial w_0}{\partial X}\frac{\partial w_0}{\partial Y} + (\frac{\partial w_1}{\partial X} + \mathrm{i}Q\,w_1)\frac{\partial \overline{w}_1}{\partial Y} + (\frac{\partial \overline{w}_1}{\partial X} - \mathrm{i}Q\,\overline{w}_1)\frac{\partial w_1}{\partial Y} \end{array} \right\} \tag{7}$$

Next, two additional simplifications will be introduced in the envelope model, in the same spirit as in [17]. First, the displacement field is reduced to a membrane mean displacement and to a bending wrinkling, i.e. $\mathbf{u}_1 = 0$, $w_0 = 0$, which means that we only consider the influence of wrinkling on a flat membrane state. Second, the deflection envelope is assumed to be real, which disregards the phase modulation of the wrinkling pattern: $w_1(X,Y)$ is real. Hence the envelope of the displacement is reduced to three components $\mathbf{u}_0 = (u_0, v_0)$ and w_1, which will be rewritten for simplicity as $(u,v) \stackrel{\text{def}}{=} (u_0, v_0)$, $w \stackrel{\text{def}}{=} w_1$. Hence the simplified version of the mean strain field is:

$$\{\gamma\} \stackrel{\text{def}}{=} \{\gamma_0\} = \left\{ \begin{array}{c} \frac{\partial u}{\partial X} + (\frac{\partial w}{\partial X})^2 + Q^2 w^2 \\ \frac{\partial v}{\partial Y} + (\frac{\partial w}{\partial Y})^2 \\ \frac{\partial u}{\partial Y} + \frac{\partial v}{\partial X} + 2\frac{\partial w}{\partial X}\frac{\partial w}{\partial Y} \end{array} \right\} \tag{8}$$

The membrane strain formula – Eq. (8) – is quite similar to the strain of the initial von Kármán model. It can be split, first, in a linear part $\varepsilon(\mathbf{u})$, which is the symmetric part of the displacement gradient and corresponds to the pure membrane strain, second to a nonlinear part $\gamma^{\mathrm{wr}}(w)$, which is more or less equivalent to the wrinkling deformation of [7] and is given by:

$$\{\gamma^{\mathrm{wr}}(w)\} = \left\{ \begin{array}{c} (\frac{\partial w}{\partial X})^2 + Q^2 w^2 \\ (\frac{\partial w}{\partial Y})^2 \\ 2\frac{\partial w}{\partial X}\frac{\partial w}{\partial Y} \end{array} \right\} \tag{9}$$

The main difference with the classical von Kármán strain is the extension $Q^2 w^2$ in the direction of the wrinkles. So, if the linear strain is compressive, wrinkling leads to a decrease of the membrane strain.

Last we apply the multiple-scale rule – Eq. (5) – to the membrane energy. This leads, for instance, to:

$$\iint\limits_{\text{period}} \gamma_X^2 \,\mathrm{d}\omega \approx \iint\limits_{\text{period}} (\gamma_{X0}^2 + 2\gamma_{X1}^2)\,\mathrm{d}\omega \approx \iint\limits_{\text{period}} \gamma_{X0}^2 \,\mathrm{d}\omega \tag{10}$$

where the first approximation is deduced from Eq. (5) and from Parseval's identity, truncated at harmonic one and the second one follows from the assumption $\mathbf{u}_1 = 0$, $w_0 = 0$. According to these rules, the membrane energy becomes:

$$2\mathcal{E}_{\mathrm{mem}}(\mathbf{u}, w) = \frac{Et}{1-\nu^2} \iint \left\{ \begin{array}{l} (\frac{\partial u}{\partial X} + (\frac{\partial w}{\partial X})^2 + Q^2 w^2)^2 + (\frac{\partial v}{\partial Y} + (\frac{\partial w}{\partial Y})^2)^2 \\ \quad + 2(1-\nu)(\frac{1}{2}(\frac{\partial u}{\partial X} + \frac{\partial v}{\partial Y}) + \frac{\partial w}{\partial X}\frac{\partial w}{\partial Y})^2 \\ \quad + 2\nu(\frac{\partial u}{\partial X} + (\frac{\partial w}{\partial X})^2 + Q^2 w^2)(\frac{\partial v}{\partial Y} + (\frac{\partial w}{\partial Y})^2) \end{array} \right\} \mathrm{d}\omega \tag{11}$$

2.4. Macroscopic bending energy

The bending energy is reduced to a macroscopic version in the same framework: $\mathbf{u}_1 = (u_1, v_1) = (0, 0)$, $w_0 = 0$, w_1 real. The identity (5) is applied to the two terms of the bending energy:

$$h = (\Delta w)^2 - 2(1-\nu)\left[\frac{\partial^2 w}{\partial X^2}\frac{\partial^2 w}{\partial Y^2} - \left(\frac{\partial^2 w}{\partial X \partial Y}\right)^2\right] = h^{\mathrm{A}} - 2(1-\nu)h^{\mathrm{B}}$$

Hence one gets (the indices 1 and −1 refer to the number m of the harmonics):

$$h_0^{\mathrm{A}} = 2(\Delta w)_1(\Delta w)_{-1} = 2\left|(\Delta w)_1\right|^2 = 2\left|\Delta w_1 - Q^2 w_1 + 2\mathrm{i}Q\frac{\partial w_1}{\partial X}\right|^2$$

Since $w = w_1$ is real, one gets:

$$h_0^{\mathrm{A}} = 2\left(\Delta w - Q^2 w\right)^2 + 8Q^2\left(\frac{\partial w}{\partial X}\right)^2 \tag{12}$$

In the same way, the second term h_0^{B} is given by:

$$h_0^{\mathrm{B}} = 2\left(\frac{\partial^2 w}{\partial X^2} - Q^2 w\right)\frac{\partial^2 w}{\partial Y^2} - 2\left(\frac{\partial^2 w}{\partial X \partial Y}\right)^2 - 2Q^2\left(\frac{\partial w}{\partial Y}\right)^2 \tag{13}$$

As in [17, §4.3], the derivatives of order three or four in the differential equations are neglected because the derivatives of order two are sufficient to define a macroscopic length scale and to recover the Landau–Ginzburg asymptotic approach. This leads to:

$$\mathcal{E}_{\mathrm{ben}}(w) = \iint \left\{Q^4 w^2 - 2Q^2 w \Delta w + 4Q^2\left(\frac{\partial w}{\partial X}\right)^2 + 2\left(1-\nu^2\right)Q^2\left[w\frac{\partial^2 w}{\partial Y^2} + \left(\frac{\partial w}{\partial Y}\right)^2\right]\right\} \mathrm{d}\omega \tag{14}$$

2.5. The full membrane-wrinkling model

The macroscopic membrane model is deduced from the total energy, which is the sum of the membrane energy – Eq. (11), of the bending energy – Eq. (14), and of the energy of the applied loads. Let us calculate the corresponding partial differential equations in the case where all the external loads are applied on the boundary. In this case, the sum of bending and membrane energies is stationary:

$$\delta\mathcal{E}_{\mathrm{ben}} + \delta\mathcal{E}_{\mathrm{mem}} = 0$$

for any virtual displacement that is zero at the boundary. This gives:

$$\delta\mathcal{E}_{\mathrm{ben}} + \iint_\omega \mathbf{N} : \delta\gamma^{\mathrm{wr}}\,\mathrm{d}\omega = 0 \tag{15}$$

$$\iint_\omega \mathbf{N} : \delta\boldsymbol{\varepsilon}\,\mathrm{d}\omega = 0 \tag{16}$$

After straightforward calculations, the differential equations of the macroscopic problem are as follows:

$$\operatorname{div}\mathbf{N} = 0 \tag{17}$$

$$\mathbf{N} = \mathbf{L}^m : \left[\boldsymbol{\varepsilon}(u) + \boldsymbol{\gamma}^{\mathrm{wr}}(w)\right] \tag{18}$$

$$-6DQ^2\frac{\partial^2 w}{\partial X^2} - 2DQ^2\frac{\partial^2 w}{\partial Y^2} + \left(DQ^4 + N_X Q^2\right)w - \operatorname{div}(\mathbf{N}\cdot\nabla w) = 0 \tag{19}$$

where the expression of the wrinkling membrane strain $\gamma^{\mathrm{wr}}(w)$ is given in Eq. (9).

2.6. Comments

1. The nonlinear model – Eqs. (17)–(19) – couples nonlinear membrane equations with a bifurcation equation – Eq. (19) – satisfied by the envelope of the wrinkling patterns. It extends the analysis of Damil and Potier-Ferry [17], who coupled a beam membrane with a one-dimensional Landau–Ginzburg equation. Hence the bifurcation equation – Eq. (19) – is a sort of bidimensional Landau–Ginzburg equation.
2. If the membrane stress is prescribed and uniform:

$$\mathbf{N} = N_X \mathbf{e}_X \otimes \mathbf{e}_X + N_Y \mathbf{e}_Y \otimes \mathbf{e}_Y$$

Eq. (19) becomes identical to a linear eigenvalue problem as in a linear buckling analysis. In the general case, the membrane stress is unknown and Eqs. (17)–(19) describe a nonlinear coupled membrane-wrinkling model that can be solved by standard numerical techniques. In this paper, an example of numerical solution is presented in Section 3.2.
3. The nonlinear model – Eqs. (17)–(19) – is consistent with two ideas used in other macroscopic membrane models. First, we have obtained a splitting between a membrane strain and a wrinkling strain, as in the well-known theory by Roddeman et al. [7]. Next, since we follow an approach consistent with Landau–Ginzburg theory, the final bifurcation equation (19) includes an internal length. As underlined in [16], the mechanical model is a generalised continuum and the stress is not reduced to the mean value of microscopic stress: the first terms of Eq. (19) contains the effect of the first Fourier coefficient of the bending moment. This can be qualitatively compared with the ideas of Banerjee et al. [12,13], who introduce an internal length via Cosserat theory.
4. The differential equations (17)–(19) seem quite different from the classical pure membrane theory, which postulates a nonlinear relation between membrane stress and strain; see for instance [5]. Nevertheless, the pure membrane theory can be consistent with a degenerate version of Eqs. (17)–(19). The latter can be obtained by dropping all derivatives in Eq. (19), which leads to $(N_X + DQ^2)w = 0$. If one transforms the latter in a perturbed bifurcation equation as:

$$\left(N_X + DQ^2\right)w = \delta \tag{20}$$

one gets the deflection as a function of one component of the membrane stress. In Eq. (20), δ is a small perturbation parameter that transforms the perfect bifurcation equation into a perturbed bifurcation one. If one simplifies the wrinkling strain – Eq. (9) – as $\gamma^{wr}(w) = Q^2 w^2 \mathbf{e}_X \otimes \mathbf{e}_X$ and if one combines Eqs. (18) and (20), one can drop the deflection and deduce a nonlinear relation between membrane strain $\boldsymbol{\varepsilon}(\mathbf{u})$ and membrane stress $\mathbf{N}$:

$$\boldsymbol{\varepsilon}(u) + \frac{Q^2\delta^2}{(N_X Q^2 + D)^2}\mathbf{e}_X \otimes \mathbf{e}_X = \left(\mathbf{L}^m\right)^{-1} : \mathbf{N} \tag{21}$$

3. Some analytical and numerical solutions

In this section, we present a few solutions of the system (17)–(19). Probably, many exact or approximated solutions of this new system can be found. In this paper, we limit ourselves, first to an analytical solution of the linearised system in order to establish the multiple-scale character of membrane wrinkling, second to some numerical solutions of the full nonlinear problem (17)–(19), to show that this macroscopic model is able to describe the evolution of wrinkles even with a coarse finite-element mesh.

3.1. An analytical solution for wrinkling initiation

Let us consider the rectangular membrane $[0, L_X] \times [0, L_Y]$ pictured in Fig. 1, which is submitted to a large uniform tensile stress $N_Y = t\sigma_Y > 0$ and to a small uniform compressive stress loading $N_X = t\sigma_X < 0$. The instability wavelength and the critical compressive stress will be deduced from the envelope equation (19). One seeks the value of the compressive stress at which wrinkling starts. The linearised version of the envelope equation (19) is rewritten as:

$$-6DQ^2\frac{\partial^2 w}{\partial X^2} - \left(2DQ^2 + t\sigma_Y\right)\frac{\partial^2 w}{\partial Y^2} + DQ^4 w = t|\sigma_X|\left(Q^2 w - \frac{\partial^2 w}{\partial Y^2}\right)$$

If the plate is clamped, it is known [19,20] that the envelope w vanishes on the boundary, what leads to a linear mode in the form:

$$w(X, Y) = \sin(\pi X/L_X)\sin(\pi X/L_Y)$$

This leads to a classical relation between compressive stress and wavenumber.

$$t|\sigma_X|(Q) = \frac{6DQ^2\frac{\pi^2}{L_X^2} + (2DQ^2 + t\sigma_Y)\frac{\pi^2}{L_Y^2} + DQ^4}{Q^2 + \frac{\pi^2}{L_X^2}} \tag{22}$$

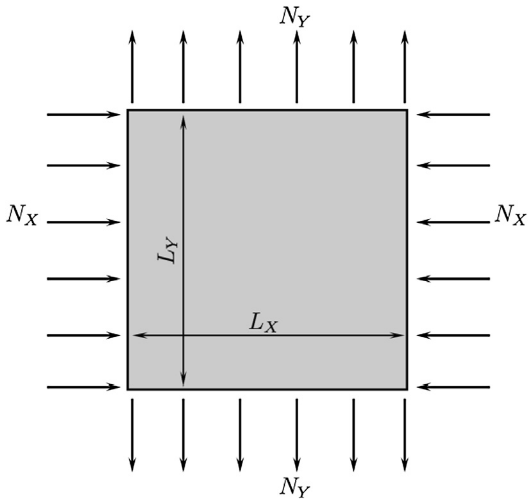

Fig. 1. Rectangular membrane under biaxial load.

Hence our approach is able to define the stability wavenumber by minimising the stress as a function of Q. For the sake of simplicity, we take into account the orders of magnitude $1 \ll QL_X$, $2DQ^2/t \approx |\sigma_X| \ll \sigma_Y$ to simplify Eq. (22) in the following manner:

$$|\sigma_X|(Q) = \frac{\sigma_Y \pi^2}{Q^2 L_Y^2} + \frac{DQ^2}{t} \tag{23}$$

The minimum of the latter yields values of the wavenumber and of the critical compressive stress that are consistent with the results of the literature [21,22]:

$$Q^{\mathrm{wr}} = \sqrt[4]{12\pi^2(1-\nu^2)}\frac{1}{\sqrt{tL_Y}}\sqrt[4]{\frac{\sigma_Y}{E}} \cong 3.2\frac{1}{\sqrt{tL_Y}}\sqrt[4]{\frac{\sigma_Y}{E}}$$

$$l^{\mathrm{wr}} = \frac{2\pi}{Q^{\mathrm{wr}}} \cong 1.95\sqrt{tL_Y}\sqrt[4]{\frac{E}{\sigma_Y}}$$

$$\left|\sigma_X^{\mathrm{wr}}\right| = \frac{\pi}{\sqrt{3(1-\nu^2)}}\sqrt{E\sigma_Y}\frac{t}{L_Y}$$

This simple calculation brings out the multiple-scale character of the wrinkling phenomenon: indeed, the wrinkling threshold depends on the wavelength, which is a microscopic quantity, but this wavelength depends on the width of the plate, which is a macroscopic length. Thus a full wrinkling analysis has to associate micro- with macro-scales.

3.2. A numerical post-bifurcation analysis for wrinkling

The partial differential system (17)–(19) has been discretized by standard finite elements. The pure membrane approach – Eqs. (17) and (21) – has also been discretized in order to evaluate the importance of the spatial derivatives of the envelope. Eight node quadrangles Q8 have been chosen. The details of the procedure will be presented elsewhere.

A thin rectangular membrane under uniaxial load (see Fig. 2) is studied, as in [23,24]. The side lengths L_X and L_Y are respectively 1400 mm and 200 mm, and the thickness t is 0.05 mm. The long sides are stress-free. Along the short sides, a uniform tensile stress is applied in the axial direction and the displacements in the X-direction are locked.

Full nonlinear analyses of this problem have been done, first by a Q8 discretisation of the new model – Eqs. (17)–(19) –, second by a Q8 discretisation of the nonlinear pure membrane model – Eqs. (17) and (21) –, last by quadratic shell elements S825 of the Abaqus code that will be considered as the reference. The nonlinear problems associated with the first two models have been solved by the Asymptotic Numerical Method [25]. In Fig. 3, one sees that the post-bifurcation patterns obtained by the new reduced model – Eqs. (17)–(19) – are quite similar to those provided by the full shell model. This establishes the relevance of this new reduced model to represent the wrinkling modes in a case with a nonuniform pre-buckling stress field.

In Fig. 4, we have plotted the maximal deflection as a function of the applied tensile load for these three models. One sees that the new reduced model – Eqs. (17)–(19) – gives about the same bifurcation point as the reference model as well as the post-bifurcation response. As expected, the number of unknowns is much smaller with the envelope models that do not describe explicitly the full details of the wrinkles. On the contrary, the pure membrane model underestimates the wrinkling

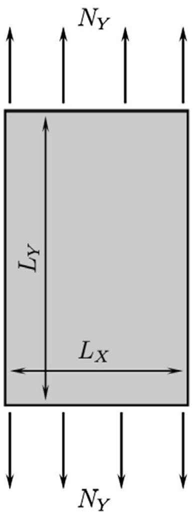

Fig. 2. A rectangular membrane under uniaxial load.

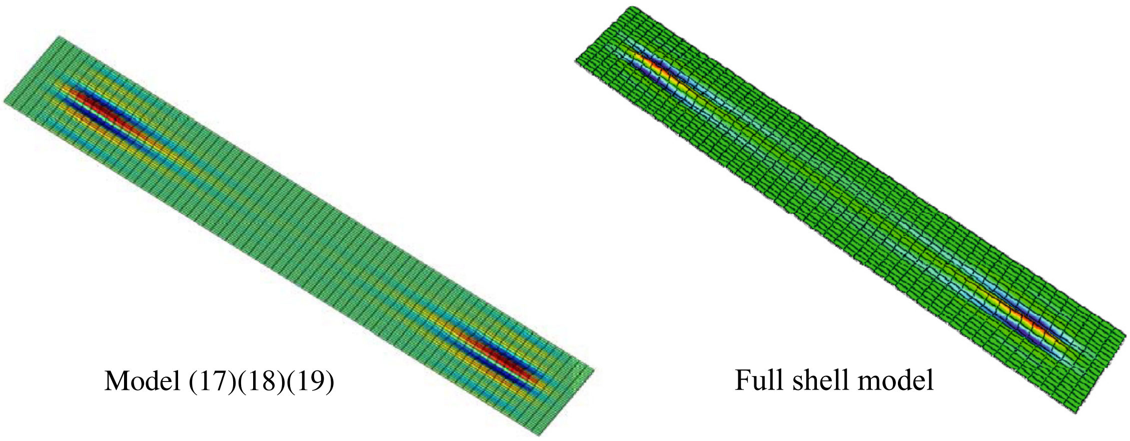

Fig. 3. Post-bifurcation patterns obtained with the envelope model and a full shell model. Colour available online.

threshold and overestimates the wrinkling amplitude. This is consistent with the analytical study of Section 3.1 that has pointed out that the bifurcation load depends strongly on a macroscopic length and that this influence of the macroscopic structure cannot be accounted for if one neglects the spatial derivatives of the envelope $w(X, Y)$. Last, a wrinkling pattern along the width is plotted in Fig. 5 for the full and the reduced model. Globally, they are quite similar, but with slight differences for the amplitude and the wavelength. In fact, the wavelength of the reference model increases slightly near the edges and this change of wavelength cannot be captured with a real envelope as in Eq. (19). Clearly, the present result could be still improved by keeping a complex envelope of the deflection as in Eq. (7).

4. Last comments

A new wrinkling model has been presented in this paper. The approach is analogous to bifurcation analyses for instability patterns via Landau–Ginzburg theory. The final model – Eqs. (17)–(19) – is simple: the first equations (17) and (18) are membrane equations including an additional wrinkling membrane strain and they are coupled with a sort of Landau–Ginzburg envelope equation – Eq. (19). For this first paper about this new macroscopic approach of membrane wrinkling, two solutions have been presented. First an analytic solution of a clamped rectangular membrane illustrates that membrane wrinkling is a multi-scale problem that requires consistent multi-scale approaches. Second, a numerical solution in a case with a nonuniform pre-buckling stress has shown the relevance of the new reduced model and the necessity of accounting for some spatial derivatives of the envelope. This approach can likely have alternative applications, for instance for thin films on a compliant substrate [26] or for flatness defects induced by rolling process [27], but this could require some modifications to account for variable wrinkle orientations.

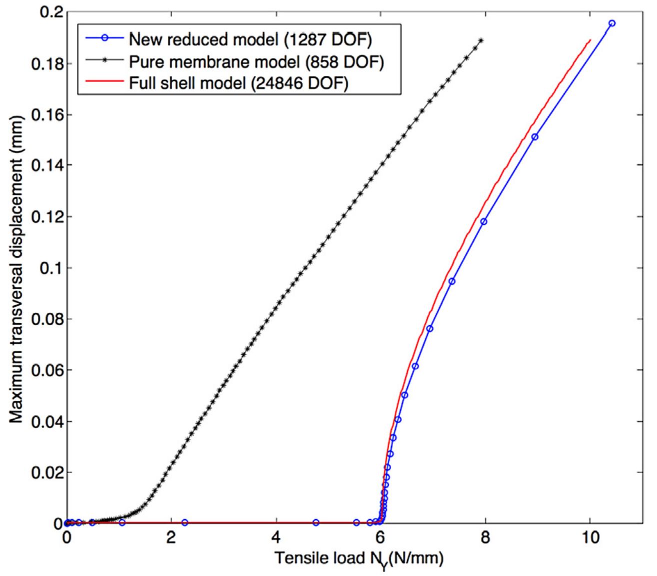

Fig. 4. Bifurcation curves for the tensile problem of Fig. 3, with three different models. Colour available online.

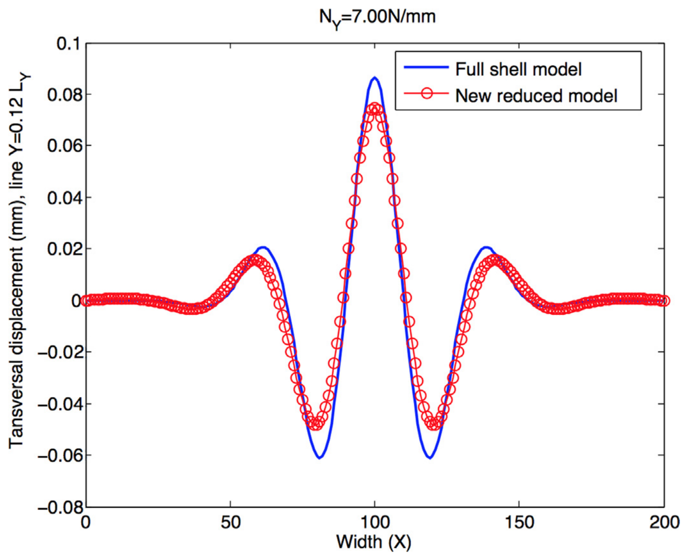

Fig. 5. Post-bifurcation profile along the width. Colour available online.

Acknowledgement

Dr. H. Hu acknowledges the support from the Science and Technology Agency of Hubei Province of China (Grant Nos. 2010BFA009 and 2011CDA047).

References

[1] Y.W. Wong, S. Pellegrino, Wrinkled membranes—Part 1: Experiments, J. Mech. Mater. Struct. 1 (2006) 3–25.
[2] C.G. Wang, X.W. Du, H.F. Tan, X.D. He, A new computational method for wrinkling analysis of gossamer space structures, Int. J. Solids Struct. 46 (2009) 1516–1526.
[3] Y. Lecieux, R. Bouzidi, Experimentation analysis on membrane wrinkling under biaxial load—Comparison with bifurcation analysis, Int. J. Solids Struct. 47 (2010) 2459–2475.
[4] Y. Lecieux, R. Bouzidi, Numerical wrinkling prediction of thin hyperelastic structures by direct energy minimization, Adv. Eng. Softw. 50 (2012) 57–68.
[5] B. Tabarrok, Z. Qin, Nonlinear analysis of tension structures, Comput. Struct. 45 (1992) 973–984.
[6] J. Rodriguez, G. Rio, J.-M. Cadou, J. Troufflard, Numerical study of dynamic relaxation with kinetic damping applied to inflatable fabric structures with extensions for 3D solid element and non-linear behavior, Thin-Walled Struct. 49 (2011) 1468–1474.
[7] D.G. Roddeman, C.W.J. Oomens, J.D. Janssen, J. Drukker, The wrinkling of thin membranes: Part 1—Theory, J. Appl. Mech. 54 (1987) 884–887.
[8] K. Lu, M. Accorsi, J. Leonard, Finite element analysis of membrane wrinkling, Int. J. Numer. Methods Eng. 50 (2001) 1017–1038.

[9] H. Schoop, L. Taenzer, J. Hornig, Wrinkling of nonlinear membranes, Comput. Mech. 29 (2002) 68–74.
[10] Y. Miyazaki, Wrinkle/slack model and finite element dynamics of membrane, Int. J. Numer. Methods Eng. 66 (2006) 1179–1209.
[11] T. Akita, T. Nakashino, M.C. Natori, K.C. Park, A simple computer implementation of membrane wrinkle behaviour via a projection technique, Int. J. Numer. Methods Eng. 71 (2007) 1231–1259.
[12] B. Banerjee, A. Shaw, D. Roy, The theory of Cosserat points applied to the analyses of wrinkled and slack membranes, Comput. Mech. 43 (2009) 415–429.
[13] N.A. Pimprikar, B. Banerjee, D. Roy, R.M. Vasu, S.R. Reid, New computational approaches for wrinkled and slack membranes, Int. J. Solids Struct. 47 (2010) 2476–2486.
[14] J.E. Wesfreid, S. Zaleski (Eds.), Cellular Structures in Instabilities, Lect. Notes Phys., vol. 210, Springer-Verlag, Heidelberg, 1984.
[15] R. Hoyle, Pattern Formation, an Introduction to Methods, Cambridge University Press, 2006.
[16] N. Damil, M. Potier-Ferry, A generalized continuum approach to describe instability pattern formation by a multiple scale analysis, C. R. Mecanique 334 (2006) 674–678.
[17] N. Damil, M. Potier-Ferry, Influence of local wrinkling on membrane behaviour: a new approach by the technique of slowly variable Fourier coefficients, J. Mech. Phys. Solids 58 (2010) 1139–1153.
[18] H. Hu, N. Damil, M. Potier-Ferry, A bridging technique to analyze the influence of boundary conditions on instability patterns, J. Comput. Phys. 230 (2011) 3753–3764.
[19] K. Mhada, B. Braikat, H. Hu, N. Damil, M. Potier-Ferry, About macroscopic models of instability pattern formation, Int. J. Solids Struct. 49 (2012) 2978–2989.
[20] Y. Liu, K. Yu, H. Hu, S. Belouettar, M. Potier-Ferry, A Fourier-related double scale analysis on instability phenomena of sandwich beams, Int. J. Solids Struct. 49 (2012) 3077–3088.
[21] E. Cerda, L. Mahadevan, Geometry and physics of wrinkling, Phys. Rev. Lett. 90 (2003) 074302.
[22] E. Cerda, K. Ravi-Chandar, L. Mahadevan, Wrinkling of an elastic sheet under tension, Nature 419 (2000) 579–580.
[23] N. Friedl, F.G. Rammerstorfer, F.D. Fisher, Buckling of stretched strips, Comput. Struct. 78 (2000) 185–190.
[24] N. Jacques, M. Potier-Ferry, On mode localisation in tensile plate buckling, C. R. Mecanique 333 (2005) 804–809.
[25] B. Cochelin, N. Damil, M. Potier-Ferry, Asymptotic-numerical methods and Padé approximants for nonlinear elastic structures, Int. J. Numer. Methods Eng. 37 (1994) 1187–1213.
[26] B. Audoly, A. Boudaoud, Buckling of a stiff film bound to a compliant substrate—Part II: A global scenario for the formation of herringbone pattern, J. Mech. Phys. Solids 56 (2008) 2422–2443.
[27] S. Abdelkhalek, P. Montmitonnet, M. Potier-Ferry, H. Zahrouni, N. Legrand, P. Buessler, Strip flatness modelling including buckling phenomena during thin strip cold rolling, Ironmak. Steelmak. 37 (2010) 290–297.